DYNAMIC MODELING OF A DEPOSITION MECHANISM OF A FREEFORM MANUFACTURING MACHINE

Eduardo Paiva Okabe, eduardo.okabe@fca.unicamp.br
UNICAMP – Universidade Estadual de Campinas
FCA - School of Applied Sciences
Rua Pedro Zaccaria, 1300 – Jardim Sta. Luiza – Limeira – SP - Brazil

Abstract. *This work shows the effect of a flexible support structure and flexible guides in a deposition mechanism adopted in free-form manufacturing machines known as FDM (fused deposition modeling). The freeform manufacturing, or rapid prototyping, has been adopted in product development, during the conceptual phase of testing, where the shapes, dimensions and connections between parts can be checked. With the introduction of more resistant materials such as ABS plastic and metals such as titanium, these freeform processes are now used in developing functional models, which behave very close to the final product. The material deposition machines operate similarly to ink jet printers, however, their heads move in two dimensions, instead of just one, to deposit the construction material of the layered model. This head usually slide on axis guides, modeled as beams, that maintains its vertical position (Z) and provide reference to the horizontal movement (X and Y). The simulation system of head, guides and structure shows that the stiffness of these guides influences the dynamic behavior of the head, affecting the material deposition and changing dimensional accuracy of the model. Increasing this stiffness causes an increase in production cost of the machine, whether applying a material with higher stiffness, or increasing the dimension of the guides, which make them heavier, therefore demanding more powerful motors. The other undesirable effect is that the support structure begin to play a significant role on the dynamics of the head. With this model of the system, we can determine the necessary combination of stiffness of the guide and support structure to achieve a specified accuracy and speed.*

Keywords*: Dynamic Simulation, Freeform Manufacturing, Elastic Components*

1. INTRODUCTION

Nowadays, companies have faced product development cycles (time-to-market) ever shorter, and their survival in this environment is closely related to fast development of new products and services, within cost and quality targets. In this competitive scenario that the application of the freeform manufacturing processes becomes vital to guide the development of new products.

It is in the prototyping phase that concepts and functional characteristics are tested, which is essential to verify design, strength and problems related to the use of the product, before the manufacturing design (Dutson, 2005). In the case of conceptual prototypes, the idea is to use the physical model to refine its shape, ergonomics and aesthetics, and possibly optimize these characteristics.

To help this prototyping process, a series of manufacturing processes was developed in order to satisfy this need in the industry. These processes are known as rapid prototyping methods (Ullman, 2008) or free-form manufacturing, given its nature to transform raw material directly into a product without the use of molds, or a long series of construction processes.

The rapid prototyping methods can be classified by the nature of their process, therefore, additive or subtractive (Cooper, 2001). Subtractive processes are established and widely used in industry such as CNC milling machines, lathes, machining centers (Mognol et al., 2007) and electrical discharge machining (EDM). Some newer processes can be included in this list, such as the laser, plasma and water cutting. These methods are characterized by removing material from a block of raw material to produce the final part. Usually they work with precision from 0.1 and 0.001 mm, and are relatively fast; however, the geometry that each process can handle is restricted, which creates a number of difficulties to create prototypes of complex geometry.

For example, a laser cutting machine usually works in a normal position to a plate surface, and for the construction of a three-dimensional model, it would require several sheets (layers), which should be attached with each other, using welding or adhesive, which would require an effort to position and to finish the plates junction, besides other problems such as warping, deformation and burr, common to this type of process. All these factors make the construction of a three-dimensional model from this process, difficult to automate and subjected to several errors.

Additive processes were developed to overcome the problems of creating complex geometry models (Cooper, 2001). Initially, these processes were applied in the construction of conceptual models, because the raw material used had low mechanical strength, which restricted the functional testing of the models. However, with the evolution of these processes, new materials have been adapted, and it is now possible to produce parts and components of great strength by using, for example, ABS plastic or titanium.

The additive processes have a precision from 0.5 mm to 0.05 mm, and are relatively slow, taking several hours or days to build the model. The raw material employed is usually expensive, because it has very well controlled characteristics, for instance, the melting point, so the accuracy is guaranteed. However, these methods deal with extremely complex geometries, which can generate at one time, several parts assembled into a single model, such as a gear train, eliminating the assembly phase of the prototype.

There are many additive processes, among them, stereolithography, selective laser sintering, melting arc, three-dimensional printing and deposition of molten material. Developed in the late '80s, the deposition of material by melting (Berridge, 2010) is characterized by the addition of molten plastic directly into the model through an extrusion head (Fortus, 2010), a process which is also known as FDM (fused deposition modeling). The model construction is made layer by layer, and a different material, which has to be easy to remove at the end of the process, is used to build models with internal spaces, or to separate components within the model. The temperature control and speed of extrusion material is one of the key points of this process, because it defines the adhesion between the layers, the uniformity of layer thickness, and surface finish of the piece. FDM has a lower cost of operation compared to the sintering and stereolithography, producing pieces of good mechanical strength; however, the polymer used is costly because it must combine the necessary strength and adhesion between layers.

Based on the FDM technology, several open projects of rapid prototyping systems have been created. The system includes the prototyping machine, the control interface and the program model generation. RepRap, Fab@home and MakerBot are examples of open projects, and they all share the same goal: provide a simple and inexpensive solution to the problem of building three-dimensional models.

The RepRap project (IDMRC, 2010) has been created by Adrian Bowyer, a professor at the University of Bath. The target of RepRap is to develop a low cost three-dimensional printer that has the capacity to self-replication. This goal had been partially achieved with the production of approximately half of the machine parts daughter, in the first version of this project, named Darwin. In the second version, Mendel, the size capacity of the machine have been improved, and thus increase the percentage of self-replication. Both versions work with a mechanism that refers to the three-dimensional printers based on inkjet technology, with movement performed by stepper motors, a set of pulleys and belts. The deposition of material is made by an extrusion head feeded with a plastic wire.

The Fab@home project was initiated by Malone and Lipson (2007) at Cornell University in 2006 to develop a prototyping machine, which users could use to manufacture their own products at home. Currently there is a global community that develops the project and its various components (Fab@home, 2010). The great advantage of open design in relation to others is the great similarity between this system (modeling program, interface electronics and prototyping machine) and the commercial rapid prototyping machines.

Analyzing these open projects, we can verify that high precision is not a goal, however, it is important to predict and improve their machine's performance to optimize their projects, and build cheaper, faster and more precise machines. To answer this question, this work proposes the development of a computational model of rapid prototyping machine, which can predict the behavior of the same for the mentioned properties: precision and speed.

2. THEORETICAL MODEL

The main system of a FDM machine is the deposition mechanism, which can be seen on Fig. 1. It is composed by several components: the deposition head, which has a plastic extruder controlled by a microprocessor; a central beam, that bears the deposition head; and the lateral beams (1 and 2) that supports the end of central beam, and are attached to the support structure.

The central beam is composed by two steel round bars, which has been modeled as one component. The deposition head moves on the bars through a anti-backlash nut coupled to a leadscrew, which is rotated by a steeper motor. This leadscrew parallel to the central beam was modeled as a kinematic constraint, therefore, its mass and stiffness have not been included in the mathematical model of the mechanism. The central beam is moved by a pair of leadscrews connected to each other by a timing belt, in order to maintain the synchronism between them. These leadscrews have been modeled as kinematic constraints, like the leadscrew of the central beam (X axis).

The model (prototype) is built on the table (Fig. 1), where the deposition head places a plastic filament which creates a layer of the model, through a combination of movements of the X and Y axes. After the completion of the layer, the table moves down allowing the building of the next layer. This model decomposition (filament tracks to build a layer, and a series of layers to build the model) is calculated by a computer program, that slices a computational solid model of the part to be built, and send all information to machine's microprocessor, that controls the stepper motors of the X, Y and Z axis, and also the motors of the deposition head.

The table movement (Z axis) is slow, easily controlled and has low frequency (one step, right before the building of a new layer), due to these characteristics this movement does not have a great influence on the precision or either the speed of the process, and have not been considered in the mathematical model presented here. This consideration has leaded to the modeling of two dimensional systems to represent the deposition mechanism, shown on Fig. 2 and 3.

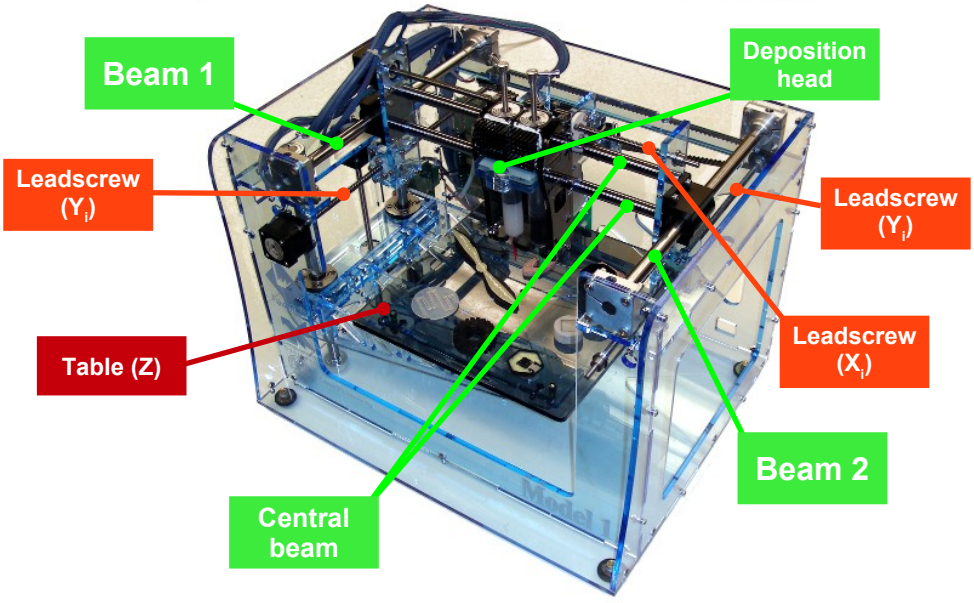

Figure 1. Fab@home prototyping machine – model 1 (Fab@home, 2010)

The model diagram of Fig. 2 has considered that the support structure of the mechanism is rigid (zero displacement); however, it has allowed the rotation of the lateral beams ends, represented by the generalized coordinates: q_1, q_2, q_3 and q_4. The central beam has had four degrees of freedom, the rotations of each end (q_5 and q_7), and axial translations (q_6 and q_8). These axial translations are determined by the bending of lateral beams (1 and 2) and axial strain of the central beam. The displacement of the central beam in the Y axis is determined by the variable y_i, which constrains the movement of the ends of central beam in this direction. The movement of the deposition head is constrained by the variable x_i relative to the central beam end connected to beam 1, which has the aforementioned coordinates (rotation q_5, axial displacement q_6 and transverse displacement y_i). The displacement in Y axis of the deposition head depends on the variable y_i and central beam bending.

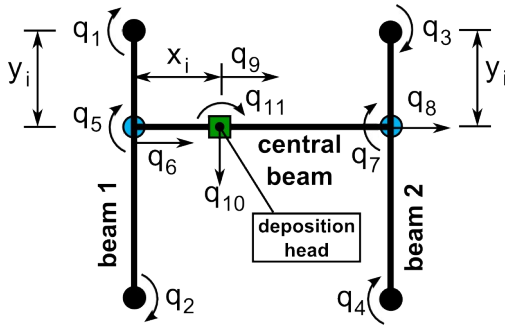

Figure 2. Model diagram of the prototyping machine with rigid support structure.

The mathematical models of deposition mechanism has been determined by a system of modified Lagrange equations (Craig, 1981), which include the constraint equations g_j:

$$\frac{d}{dt}\left(\frac{\partial T}{\partial \dot{q}_i}\right)-\frac{\partial T}{\partial q_i}+\frac{\partial V}{\partial q_i}-\sum \lambda_j \frac{\partial g_j}{\partial q_i}=Q_i \tag{1}$$

$$g_j(t, q, x_i, y_i)=0 \tag{2}$$

Where t is the time, q_i is the i_{th} generalized coordinate, T is the kinetic energy, V is the potential energy, λ_j is the j_{th} Lagrange multiplier, g_j is the j_{th} constraint equation, Q_i is the dissipative force, and dot (·) represents the time derivative.

The three beams of the mechanism (lateral 1, lateral 2 and central) are elastic components, therefore, they have been modeled using the Bernoulli-Euler formulation, that accounts bending and axial strain effects. Each one of the nodes (ends of the beam) has three degrees of freedom (DOF): two translations and one rotation.

The potential and kinetic energy of a beam related to the axial strain, can be described as:

$$V = \frac{1}{2}\int_0^L EA\left(\frac{\partial u}{\partial x}\right)^2 dx \quad \text{and} \quad T = \frac{1}{2}\int_0^L \rho A \dot{u}^2 dx \tag{3}$$

Where L is the length of the beam, E is the elasticity modulus of the beam's material, A is the beam transverse area, u is the axial motion along the beam, x is the axial coordinate, ρ is the density of the beam's material, and dot $(\cdot)$ represents the time derivative.

The potential and kinetic energy of a beam related to the bending, can be described as:

$$V = \frac{1}{2}\int_0^L EI\left(\frac{\partial^2 v}{\partial x^2}\right)^2 dx \quad \text{and} \quad T = \frac{1}{2}\int_0^L \rho A \dot{v}^2 dx \tag{4}$$

Where I is the area moment of inertia of the transverse section of the beam, v is the transverse motion along the beam, and dot $(\cdot)$ represents the time derivative.

Developing the dynamic equations of the beam, and adding a proportional damping (Ewins, 1995), they become:

$$[M]\{\ddot{q}_i\} + (\alpha[M] + \beta[K])\{\dot{q}_i\} + [K]\{q_i\} + \sum \lambda_j \left\{\frac{\partial g_j}{\partial q_i}\right\} = \{0\} \tag{5}$$

Where M is the mass matrix, K is the stiffness matrix, α is the damping coefficient related to the mass matrix, and β is the damping coefficient related to the stiffness matrix.

Energy equations of axial strain and bending generates different coefficients in the mass and stiffness matrix. The coefficients related to the axial strain can be determined through the following equations:

$$m_{ij} = \int_0^L \rho A \phi_i \phi_j dx \quad \text{and} \quad k_{ij} = \int_0^L EA \frac{\partial \phi_i}{\partial x}\frac{\partial \phi_j}{\partial x} dx \tag{6}$$

Where ϕ represents the following shape functions:

$$\phi_1(x) = 1 - \frac{x}{L} \quad \text{and} \quad \phi_2(x) = \frac{x}{L} \tag{7}$$

The function ϕ_1 is associated to the axial displacement of the node 1, and ϕ_2 is associated to the axial displacement of node 2. The coefficients related to the bending strain can be determined by:

$$m_{ij} = \int_0^L \rho A \psi_i \psi_j dx \quad \text{and} \quad k_{ij} = \int_0^L EI \frac{\partial^2 \psi_i}{\partial x^2}\frac{\partial^2 \psi_j}{\partial x^2} dx \tag{8}$$

Where ψ represents the following shape functions:

$$\psi_1 = 1 - 3\left(\frac{x}{L}\right)^2 + 2\left(\frac{x}{L}\right)^3 \;;\; \psi_2 = x - 2L\left(\frac{x}{L}\right)^2 + L\left(\frac{x}{L}\right)^3 \;;\; \psi_3 = 3\left(\frac{x}{L}\right)^2 - 2\left(\frac{x}{L}\right)^3 \tag{9}$$
$$\text{and} \quad \psi_4 = -L\left(\frac{x}{L}\right)^2 + L\left(\frac{x}{L}\right)^3$$

The function ψ_1 is associated to the transverse motion of the node 1, ψ_2 is associated to the slope (rotation) of node 1, ψ_3 is associated to the transverse motion of the node 2, and ψ_4 is associated to the slope of node 2.

The equations of the deposition head are:

$$\begin{bmatrix} m_h & 0 & 0 \\ 0 & m_h & 0 \\ 0 & 0 & Izz_h \end{bmatrix} \begin{Bmatrix} \ddot{q}_9 \\ \ddot{q}_{10} \\ \ddot{q}_{11} \end{Bmatrix} + \sum \lambda_j \begin{Bmatrix} \frac{\partial g_j}{\partial q_9} \\ \frac{\partial g_j}{\partial q_{10}} \\ \frac{\partial g_j}{\partial q_{11}} \end{Bmatrix} = \begin{Bmatrix} 0 \\ 0 \\ 0 \end{Bmatrix} \tag{10}$$

Where m_h is the mass of deposition head, Izz_h is the mass moment of inertia in Z axis of deposition head, q_9 and q_{10} are the translational coordinates, and q_{11} is the rotation of the deposition head. The constraint equations provide the mathematical representation of the physical connections between the elements, and it also supply the displacements imposed by the leadscrews. The constraint equations related to the model of Fig. 2 are:

$$\begin{aligned}
g_1 &= -q_6 + \psi_2(y_i)\cdot q_1 + \psi_4(y_i)\cdot q_2 = 0 \\
g_2 &= q_5 + \frac{\partial \psi_2(y_i)}{\partial y_i}\cdot q_1 + \frac{\partial \psi_4(y_i)}{\partial y_i}\cdot q_2 = 0 \\
g_3 &= -q_8 + \psi_2(y_i)\cdot q_3 + \psi_4(y_i)\cdot q_4 = 0 \\
g_4 &= q_7 + \frac{\partial \psi_2(y_i)}{\partial y_i}\cdot q_3 + \frac{\partial \psi_4(y_i)}{\partial y_i}\cdot q_4 = 0 \\
g_5 &= -q_9 + q_6 + x_i = 0 \\
g_6 &= q_{10} + y_i + \psi_2(x_i)\cdot q_5 + \psi_4(x_i)\cdot q_7 = 0 \\
g_7 &= q_{11} + \frac{\partial \psi_2(x_i)}{\partial x_i}\cdot q_5 + \frac{\partial \psi_4(x_i)}{\partial x_i}\cdot q_7 = 0
\end{aligned} \tag{11}$$

The constraint equations (Eq. 11) g_1, g_2, g_3, and g_4 represent the kinematic relations among lateral beams, leadscrews (y_i) and central beam. Equations g_5, g_6 and g_7 describe the kinematic relations among central beams, leadscrew (x_i) and deposition head.

Equations 5 and 11 determine the mathematical model of Fig. 1, which is deposition mechanism supported by a rigid support structure that constrains the translations of the lateral beam ends, but not the rotations (q_1, q_2, q_3 and q_4). To verify the influence of a flexible support structure, stiffness and damping coefficients have been added to the equations of the lateral beams, and a diagram of this new model can be seen on Fig. 3, which is a more realistic model of the prototyping machine shown on Fig. 1.

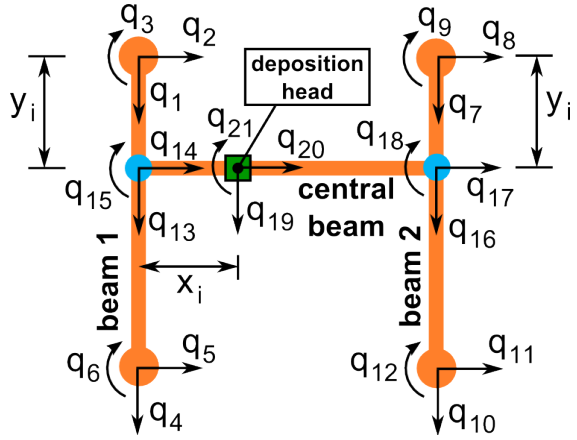

Figure 3. Model diagram of the prototyping machine with flexible support structure.

The equations of the lateral beams including the support structure flexibility are:

$$[M]\{\ddot{q}_i\}+\left(\alpha[M]+\beta[K]+\beta_S[K_S]\right)\{\dot{q}_i\}+\left([K]+[K_S]\right)\{q_i\}+\sum\lambda_j\left\{\frac{\partial g_j}{\partial q_i}\right\}=\{0\} \tag{12}$$

Where K_S is the stiffness matrix of the support structure, and β_S is the proportional damping coefficient of the support structure.

The inclusion of the support structure flexibility has increased the system freedom, therefore, increasing the number of generalized coordinates, which can be seen on Fig. 3. The constraint equations have been also modified to account these new coordinates, and have been rewritten as:

$$\begin{aligned}
g_1&=-q_{14}+\psi_1(y_i)\cdot q_2+\psi_2(y_i)\cdot q_3+\psi_3(y_i)\cdot q_5+\psi_4(y_i)\cdot q_6=0\\
g_2&=-q_{15}+\frac{\partial\psi_1(y_i)}{\partial y_i}\cdot q_2+\frac{\partial\psi_2(y_i)}{\partial y_i}\cdot q_3+\frac{\partial\psi_3(y_i)}{\partial y_i}\cdot q_5+\frac{\partial\psi_4(y_i)}{\partial y_i}\cdot q_6=0\\
g_3&=-q_{17}+\psi_1(y_i)\cdot q_8+\psi_2(y_i)\cdot q_9+\psi_3(y_i)\cdot q_{11}+\psi_4(y_i)\cdot q_{12}=0\\
g_4&=-q_{18}+\frac{\partial\psi_1(y_i)}{\partial y_i}\cdot q_8+\frac{\partial\psi_2(y_i)}{\partial y_i}\cdot q_9+\frac{\partial\psi_3(y_i)}{\partial y_i}\cdot q_{11}+\frac{\partial\psi_4(y_i)}{\partial y_i}\cdot q_{12}=0\\
g_5&=-q_{13}+q_1+y_i\\
g_6&=-q_{16}+q_7+y_i\\
g_7&=-q_{19}+\psi_1(x_i)\cdot q_{13}-\psi_2(x_i)\cdot q_{15}+\psi_3(x_i)\cdot q_{16}-\psi_4(x_i)\cdot q_{18}=0\\
g_8&=-q_{21}+\frac{\partial\psi_1(x_i)}{\partial x_i}\cdot q_{13}-\frac{\partial\psi_2(x_i)}{\partial x_i}\cdot q_{15}+\frac{\partial\psi_3(x_i)}{\partial x_i}\cdot q_{16}-\frac{\partial\psi_4(x_i)}{\partial x_i}\cdot q_{18}=0\\
g_9&=-q_{20}+q_{14}+x_i
\end{aligned} \tag{13}$$

The constraint equations (Eq. 13) g_1, g_2, g_3, g_4, g_5, and g_6 represent the kinematic relations among lateral beams, leadscrews (y_i) and central beam. Equations g_7, g_8 and g_9 describe the kinematic relations among central beams, leadscrew (x_i) and deposition head. Equations 12 and 13 determine the mathematical model of the deposition mechanism on flexible supports.

3. SIMULATION AND RESULTS

The equations presented in the former section were implemented in the OpenModelica (Fritzson, 2010), which is a simulation environment based on the Modelica language standard (Modelica, 2010). OpenModelica can solve differential-algebraic equations, which is particularly useful in modeling and simulation of mechanisms, and it employs the DASSL integrator (Brenan et al., 2000).

The parameters of the simulation and machine dimensions were based on the Fab@home model 1 project, which provide a good basis for the analysis, since all informations are available on the internet. In this machine, the lateral and central beams are made of steel (E = 210 GPa; ρ = 7850 kg/m³), and have a length of 300 mm supported by acrylic structures. These structures were introduced as L-beams in the model with the flexible support structure (Fig. 3) These beams are made of acrylic (E = 3.2 GPa; ρ = 1200 kg/m³), with a dimension of 50 by 50 mm, thickness of 5 mm and length of 300 mm. The calculated direct stiffness coefficients (part of K_S) of each beam were 297 kN/m, and considering a damping coefficient β_S equals to 0.1, the direct damping coefficients were equal to 29.7 kNs/m. The cross stiffness and cross damping coefficients of the support structure were considered null. The deposition head was modeled as rigid body with mass of 0.2 kg and mass moment of inertia of 0.01 kg·m².

The central and lateral beams of the deposition mechanism of Fab@home machine have a diameter of 10 mm; however, the simulations employed four different diameters (5, 10, 15 and 20 mm) to show the influence of this parameter, while the damping coefficient β was considered to be equal to 0.1 during all simulations. Another important parameter is the deposition head speed, which is about 5 mm/s for the Fab@home machine, but the stepper employed

(HaydonKerk E35H4B) in this machine can reach a top speed of 10 mm/s, therefore, four speeds (5, 10, 20 and 50 mm/s) were used in the simulations.

The third analysed parameter was the support structure stiffness. The rigid structure were simulated using the model of Fig. 2, and it considered that there is no displacement on the lateral beam ends. The flexible structure, model of Fig. 3, used three different stiffness coefficients (29.7 kN/m, 297 kN/m and 2970 kN/m), but the damping coefficient was kept constant ($\beta_S = 0.1$).

The trajectory that had to be followed by the deposition head was a circle with diameter of 20 mm, and the center of this circle was set in the center of the machine ($x_0 = 150$ mm and $y_0 = 150$ mm) to avoid a response asymetry due to the stiffness difference, caused by different positions of the bearings on lateral beams, which is the same effect caused by the finger tip position on a guitar string (different position equals to different pitch).

The circular trajectory was repeated ten times for each test, which leaded to a total test run of about 628 mm. Then precision could be calculated through the deviation of deposition head from the proposed trajectory, as described by the Eq. 14:

$$deviation = \sqrt{(q_9 - x_0)^2 + (q_{10} - y_0)^2} - radius \qquad \text{(rigid support structure)} \tag{14}$$

$$deviation = \sqrt{(q_{20} - x_0)^2 + (q_{19} - y_0)^2} - radius \qquad \text{(flexible support structure)}$$

Where *deviation* is the deviation of the deposition head, *radius* is the radius of the circular trajectory (10 mm), x_0 is position of the center of the trajectory in the axis X, y_0 is position of the center of the trajectory in the axis Y, and q_i are the coordinates of the deposition head.

3.1 Simulation of the deposition supported by a rigid structure

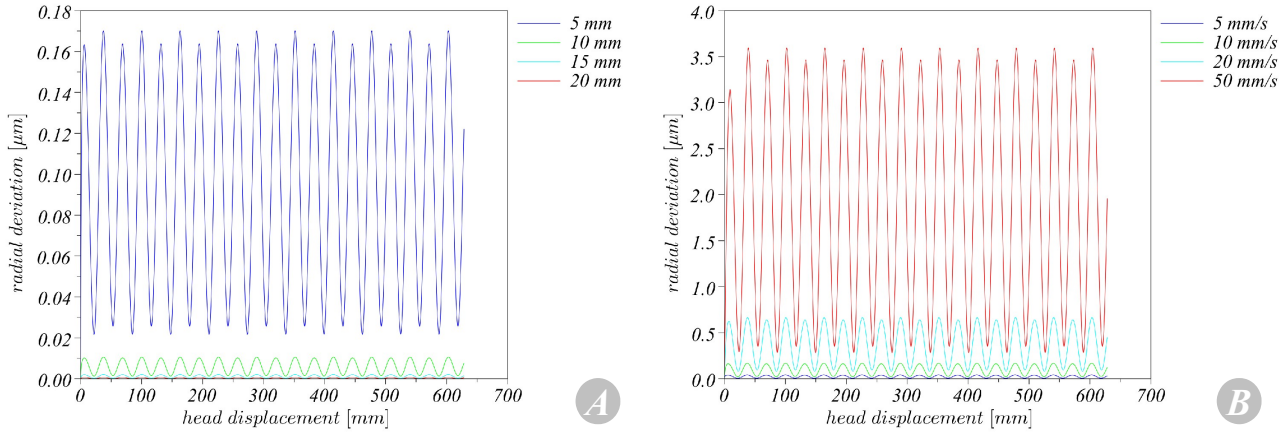

Figure 4. Deviation of the deposition head of the machine on a rigid support structure for different beam diameters (fig. 4A) and different movement speeds (fig. 4B).

Figure 4 (A and B) shows the deviation (Eq. 14) of the deposition head considering different beam diameters and movement speeds. Results shown on Fig. 4A for beam diameters of 5, 10, 15 and 20 mm, used a movement speed of 10 mm, which is close to the top speed of Fab@home model 1. It can be noticed that even the smallest diameter (5 mm) presents a very low deviation (maximum of 0.17 μm), and the deviation increases twice during the completion of one circle, and then twenty peaks can be seen on the Fig. 4A, related to the ten circles traced by the deposition head during its total trajectory.

Figure 4B shows the deviation for movement speeds of 5, 10, 20 and 50 mm/s with the deposition mechanism composed by beams of Ø 10 mm, which is the standard size of the beams for model 1 of Fab@home. The deviation is also low (less than 3.6 μm), even considering a top speed of 50 mm/s. Fab@home machine uses a stepper motor connected to a leadscrew that can reach a maximum precision of 150 μm; therefore, deviations caused by the flexibility of its components are more than forty times lower than precision that the system stepper-leadscrew can achieve.

Figure 5A shows the trajectory of the deposition head with a mechanism with Ø 10 mm beams and speed of 10 mm/s. To highlight the deviation, it was amplified 10^5 times. So it becomes clear the points where the deviation is higher, and as observed on Fig. 4, there are two points where it happens. The same behavior is observed for system with Ø 5 mm beams and speed of 50 mm/s; however, in this case, the deviation is higher than the previous case, then the amplification factor used was lower (10^3 times).

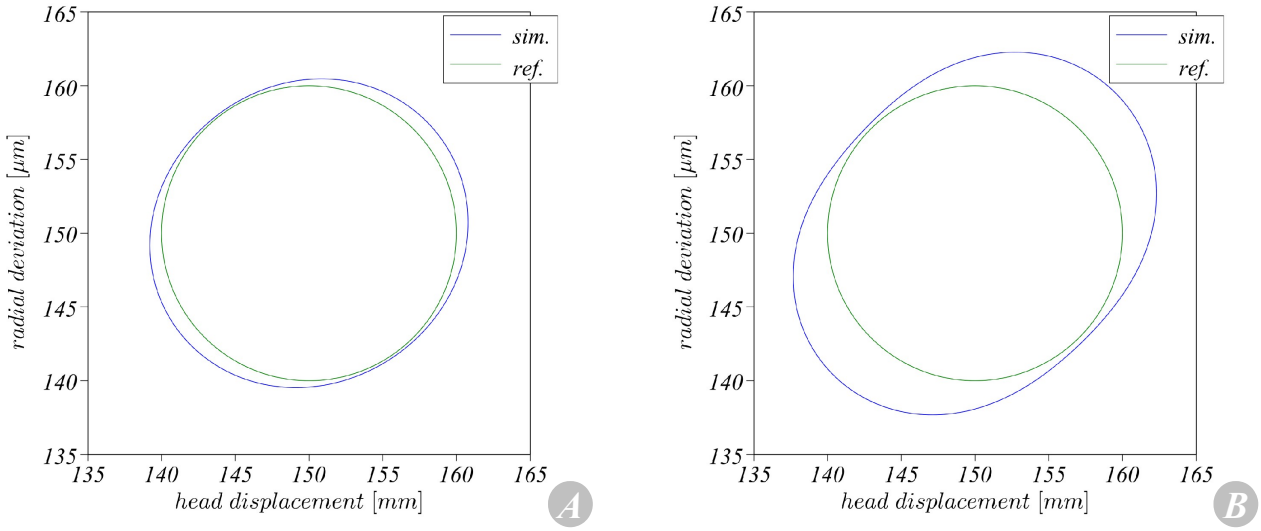

Figure 5. Trajectory reference (green) and simulated (blue) with deviation amplified 10^5 times for a system with Ø 10 mm beams and speed of 10 mm/s (fig. A), and deviation amplified 10^3 times for a system with Ø 5 mm beams and speed of 50 mm/s (fig. B).

3.2 Simulation of the deposition supported by a flexible structure

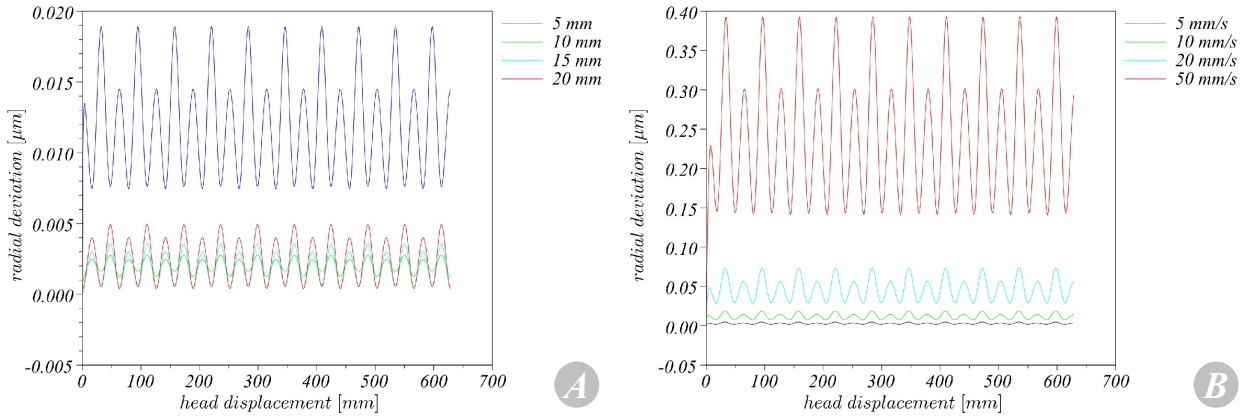

Figure 6. Deviation of the deposition head of the machine on a flexible support structure for different beam diameters (fig. 6A) and different movement speeds (fig. 6B).

Figure 6 (A and B) shows the deviation of the deposition head considering different beam diameters (5, 10, 15 and 20 mm) and movement speeds (5, 10, 20 and 50 mm/s), which are the same conditions of the system with the rigid support structure (Fig. 4 and 5). The flexible structure used in this simulation had a stiffness of 297 kN/m, as previously reported in this work.

Fig. 6A shows that considering the flexibility of the support structure reduces the deviation of the deposition head, and it results a maximum deviation of 0.019 μm in the most flexible configuration (beam diameter of 5 mm). On Fig. 6B, a maximum deviation of less than 0.4 μm in the highest speed (50 mm/s) can be seen. This lower deviation can be explained by the fact that the energy used to move the deposition head is more likely to translate the beams, instead of bending them, reducing the distortion of the deposition mechanism.

Figure 7A shows trajectory of the deposition head with a mechanism supported by a flexible structure with Ø 10 mm beams and speed of 10 mm/s, and because the deviation is lower than the machine on a rigid structure, a higher amplification factor (10^6) was employed, that highlights a change in the deviation, which is more even, and have different positions for the deviation peaks (top and bottom) in comparison to the rigid structure.

Figure 7B shows trajectory of the deposition head with a mechanism supported by a flexible structure with Ø 5 mm beams and speed of 50 mm/s, and it also shows a lower deviation in comparison to the rigid structure system, in this case, a higher amplification factor (10^4) had to be employed. The deviation is also even, but the deviation peaks are positioned on the left and on the right.

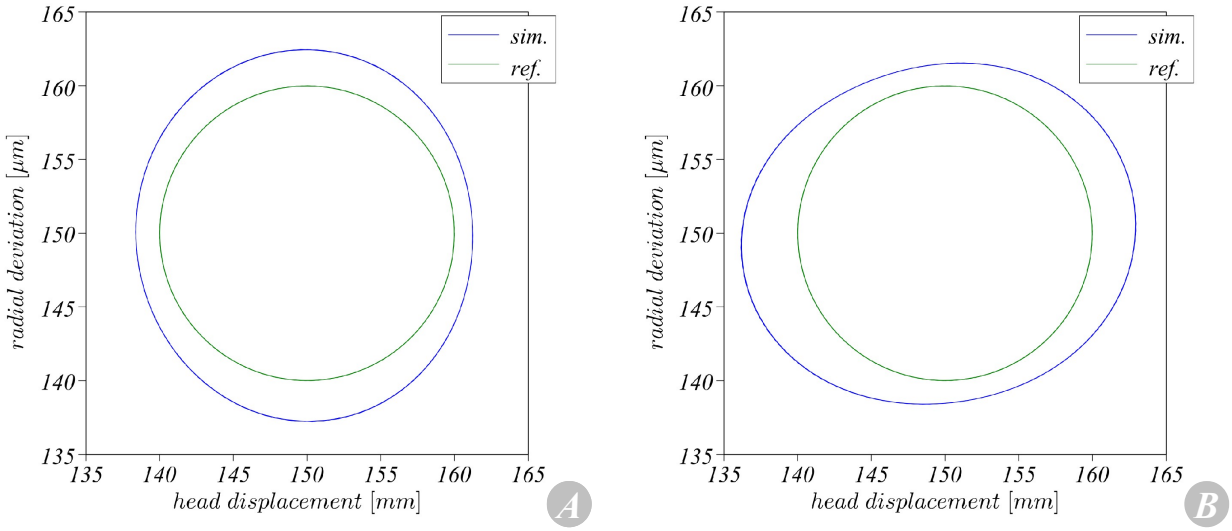

Figure 7. Trajectory reference (green) and simulated (blue) with deviation amplified 10^6 times for a system with Ø 10 mm beams, flexible support structure and speed of 10 mm/s (fig. A), and deviation amplified 10^4 times for a system with Ø 5 mm beams, flexible support structure and speed of 50 mm/s (fig. B).

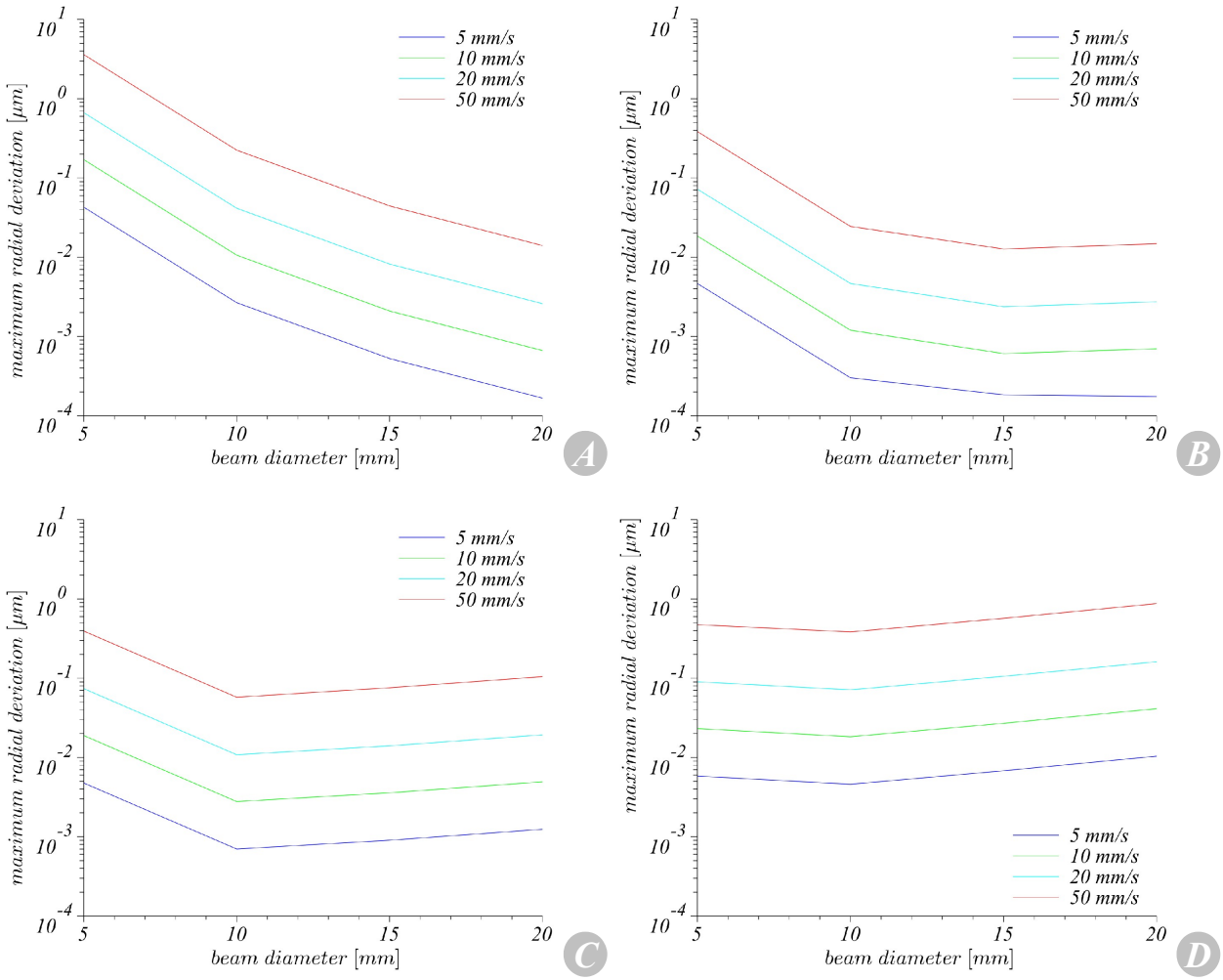

Figure 8. Maximum deviation for different stiffnesses of the support structure (A – Rigid, B – 2970 kN/m, C – 297 kN/m and D – 29.7 kN/m).

Figure 8 (A, B, C and D) shows the maximum deviation of the deposition head for different stiffnesses of the support structure.

Fig. 8A shows that the deviation increases as the speed increases, which was observed on Fig 4B, and also when the beam diameter decreases. Analysing Fig 8B, it can be observed that in a flexible structure (2970 kN/m) the reduction of the diameter brings a lower increase of the deviation. Figure 8C shows that using a more flexible support (297 kN/m), as the size of the beam increases, the deviation can also increase, due to the fact that the masses of the beams and the necessary force to move them increases. Figure 8D shows that the system with 10 mm beams still presents lower deviations, but the most flexible support simulated (29.7 kN/m) increases the deviation in all conditions, meaning that the flexibility of the support structure is more relevant to determine the system's dynamic behavior in this case than the previous ones.

4. CONCLUSION

The simulation of the deposition mechanism of a free-form manufacturing machine showed that a correct specification of the support beams and support structure can lead to a higher precision. It can also help to lower costs using thinner beams, or more flexible structures, that are usually cheaper, and still keep the machine's precision specification, which is the case of the simulated machine (Fab@home model 1), where its components can be changed without affecting its target precision (0.1 mm).

The analysis of results showed that deviation presented a frequency twice higher than the circular movement, which was quite evident in the simulation of machine supported by a rigid structure. This phenomenon can be explained by the fact that lateral beams vibrate in synchrony on their first flexible mode (ends constrained) forcing the central beam to vibrate on its second model, generating the aforementioned frequency. The simulation of the model supported by a flexible structure showed that this structure can have a great influence on the dynamic behavior of this kind of machine, and it was observed that a stiffer structure can result in less precision.

5. ACKNOWLEDGEMENTS

The author would like to thank FAPESP, Unicamp and CNPq for the support for this work. .

6. REFERENCES

Berridge, E., 2010, “HP to release a 3D printer”, The Inquirer, 20 jan. 2010, <www.theinquirer.net /inquirer/news/1587908/hp-releases-3d-printer>.

Brenan, K.E., Campbell, S.L., Petzold, L.R., 2000, “Numerical Solution of Initial-Value Problems in Differential-Algebraic Equations”, Ed. SIAM – Society for Industrial and Applied Mathematics, Philadelphia, USA, 256 p.

Chua, C. K., Leong, K. F., Lim, C. S., 2003, “Rapid prototyping : principles and applications”, World Scientific, New Jersey, USA, 392 p.

Cooper, K. G., 2001, “Rapid Prototyping Technology: Selection and Application”, Marcel Dekker, New York, USA, 248 p.

Craig, R.R, 1981, “Structural Dynamics, Introduction to Computer Methods”, Ed. John Wiley, New York, USA, 527 p.

Dutson, A. J., Wood, K. L., 2005, “Using rapid prototypes for functional evaluation of evolutionary product designs”, Rapid Prototyping Journal, v. 11 (3), pp. 126-131.

Ewins, D.J., 1995, “Modal Testing: Theory and Practice”, Research Studies Press, Somerset, UK, 313 p.

Fab@home, 2010, “Fab@home Project”, january 2010, <www.fabathome.org/wiki/ index.php/Main_Page>.

Fortus, 2010, “Prototyping using Fortus 3D Production Systems”, january 2010, <www.fortus.com/prototyping.aspx>.

Fritzson, P., 2010, “OpenModelica Users Guide – Version 2010-12-17”, december 2010, <http://www.ida.liu.se/labs/pelab/modelica/OpenModelica/releases/1.6.0/doc/OpenModelicaUsersGuide.pdf>

IDMRC - Innovative Design and Manufacturing Research Centre, 2010, “RepRap – the Replicating Rapid Prototyper Project”, january 2010, disponível em <www.bath.ac.uk/idmrc/themes/projects/amps/AMPS-Project-RepRap.pdf>.

Malone, E., Lipson, H., 2007, “Fab@Home: the personal desktop fabricator kit”, Rapid Prototyping Journal, v. 13 (4), pp 245-255.

Meriam, J.L., 1966, “Dynamics”, Ed. John Wiley, New York, USA, 387 p.

Modelica Association, 2010, “Modelica® - A Unified Object-Oriented Language for Physical Systems Modeling – Language Specification – Version 3.2”, april 2010, <https://www.modelica.org/documents/ModelicaSpec32.pdf>

Mognol, P., Rivette, M., Jégou, L., Lesprier, T., 2007, “A first approach to choose between HSM, EDM and DMLS processes in hybrid rapid tooling”, Rapid Prototyping Journal, v. 13 (1), pp. 7–16.

Santos, I.F., 2001, “Dinâmica de Sistemas Mecânicos – Modelagem, Simulação, Visualização, Verificação”, Ed. Makron Books, São Paulo, Brazil, 272 p.

7. RESPONSIBILITY NOTICE

The author is the only responsible for the printed material included in this paper.